Aerodynamic and Aeroacoustic Properties of Flatback Airfoils

Dale E. Berg* and Jose R. Zayas†
Sandia National Laboratories‡
Albuquerque, NM 87185-1124 USA

In 2002, Sandia National Laboratories (SNL) initiated a research program to demonstrate the use of carbon fiber in wind turbine blades and to investigate advanced structural concepts through the Blade Systems Design Study, known as the BSDS. One of the blade designs resulting from this program, commonly referred to as the BSDS blade, resulted from a systems approach in which manufacturing, structural and aerodynamic performance considerations were all simultaneously included in the design optimization. The BSDS blade design utilizes "flatback" airfoils for the inboard section of the blade to achieve a lighter, stronger blade. Flatback airfoils are generated by opening up the trailing edge of an airfoil uniformly along the camber line, thus preserving the camber of the original airfoil. This process is in distinct contrast to the generation of truncated airfoils, where the trailing edge the airfoil is simply cut off, changing the camber and subsequently degrading the aerodynamic performance. Compared to a thick conventional, sharp trailing-edge airfoil, a flatback airfoil with the same thickness exhibits increased lift and reduced sensitivity to soiling. Although several commercial turbine manufacturers have expressed interest in utilizing flatback airfoils for their wind turbine blades, they are concerned with the potential extra noise that such a blade will generate from the blunt trailing edge of the flatback section. In order to quantify the noise generation characteristics of flatback airfoils, Sandia National Laboratories has conducted a wind tunnel test to measure the noise generation and aerodynamic performance characteristics of a regular DU97-300-W airfoil, a 10% trailing edge thickness flatback version of that airfoil, and the flatback fitted with a trailing edge treatment. The paper describes the test facility, the models, and the test methodology, and provides some preliminary results from the test.

I. Introduction

The design innovations of the Blade Systems Design Study (BSDS) blade were made possible by a system design approach. With such an approach, the design of all elements of the system – aerodynamics, structure, and manufacturing – are optimized collectively rather than letting one design consideration control the others[1]. The system design approach led the designers of the BSDS to utilize flatback airfoils for the inboard portion of the blade. Figure 1 illustrates how these airfoils are used in a blade design. The full thickness of the flatback tapers from its maximum near the blade to a conventional, sharp trailing edge somewhere inboard of 40% of blade span. Flatback airfoils are generated by opening up the trailing edge of the airfoil uniformly along the camber line, as shown in Figure 2, thus preserving the camber of the original airfoil. This is in distinct contrast to truncated airfoils where the trailing edge of the airfoil is simply cut off, changing the camber and degrading the aerodynamic performance. Compared to a thick conventional, sharp trailing-edge airfoil, a flatback airfoil with the same thickness exhibits increased lift and reduced sensitivity to soiling, according to Standish[2]. In addition, the use of flatback airfoils permits the use of increased thickness airfoils without the chord increases that would occur if conventional thick airfoils were used. Avoiding this additional chord length makes the resulting structural design simpler and easier to build, resulting in a blade that is easier to transport[3].

These benefits do not come without risks, however, as there may be issues and concerns associated with aeroacoustics, excess drag, and three-dimensional flow along the trailing edge. The issue of acoustic emission from the flatback airfoils should be mitigated by their inboard location where airspeeds are low. Given that these airfoils

* Principal Member of Technical Staff, Wind Energy Technology Department, MS 1124, Associate Fellow AIAA
† Manager, Wind Energy Technology Department, MS 1124
‡ Sandia is a multiprogram laboratory operated by Sandia Corporation, a Lockheed Martin Company, for the United States Department of Energy's National Nuclear Security Administration under contract DE-AC04-94AL85000.

are designed for use on the inner portion of the blade (r/R<0.5) and noise generation scales as V^5 , according to Brooks, Pope and Marcolini[4], any noise produced will be attenuated by at least a factor of 2^5(=32) compared to noise produced at the tip. Brooks, *et al*[4] do present an empirical relationship for estimating the effects of trailing edge thickness (called "bluntness" by Brooks, *et al*[4]) on noise generation, but the maximum degree of trailing edge thickness for which they have data is approximately 1% of chord; an order of magnitude lower than what is apt to be encountered with the use of flatback airfoils. Trailing edge devices such as those shown in Figure 3 have been shown to be effective in addressing the excess drag and three-dimensional flow issues[5].

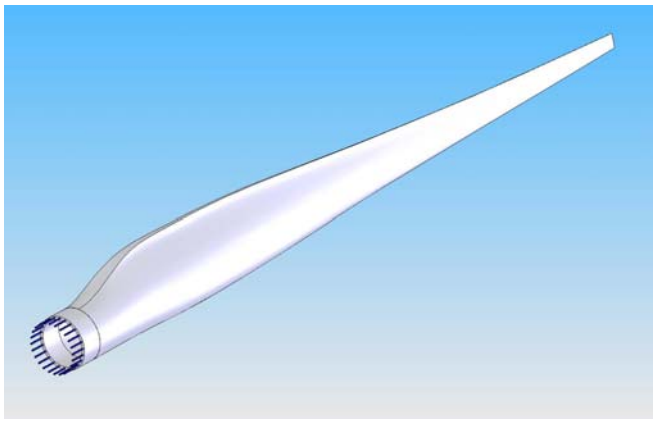

Figure 1: Typical wind turbine rotor blade incorporating a flatback airfoil. Notice that the flat trailing edge at the root tapers to a sharp trailing edge by 40% of span.

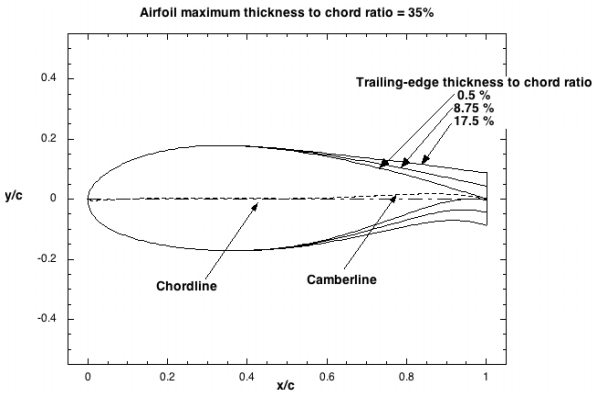

Figure 2: Flatback Airfoil

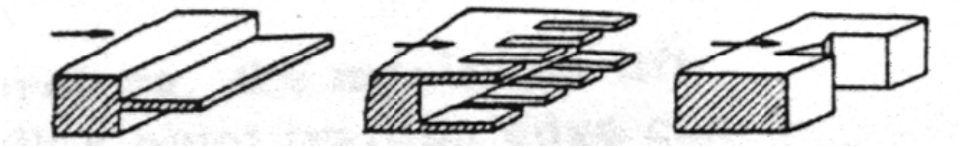

Figure 3: Possible Trailing Edge Treatments to Reduce Drag

Previous work has demonstrated that utilizing flatback airfoils in the root area of a wind turbine blade can result in decreases in blade weight and cost, both critical issues for the next generation of wind turbine blades[6]. Several commercial turbine manufacturers have expressed interest in utilizing flatback airfoils for their wind turbine blades designs, but they are always very concerned about the potential extra noise that such a blade will generate from the blunt trailing edge of the flatback section. Existing analytical tools are not capable of accurately predicting the magnitude or character of this noise.

In order to quantify the noise generation and aerodynamic performance characteristics of flatback airfoils, Sandia National Laboratories has conducted a wind tunnel test to compare the noise generation of a regular DU97-300-W airfoil[7,8], a 10% trailing edge thickness flatback version of that airfoil, and the flatback modified by the addition of a trailing edge splitter plate.

II. Test Facility, Models and Test Methodology

A. Test Facility

All of the tests presented in this paper were performed in the Virginia Tech Stability Wind Tunnel, a continuous, single return, subsonic wind tunnel with a 1.83-m (6-ft) square, 7.3-m (24-ft) long removable rectangular test section. The general layout of the tunnel is illustrated in Figure 4.

The tunnel is powered by a 0.45-MW variable speed DC motor driving a 4.3-m (14-ft) 8-bladed propeller at up to 600 rpm. This provides a maximum speed in the test section of about 80 m/s (170 mph) and a Reynolds number per meter of 5,300,000 for the models presented in this paper. Flow through the empty test section is both closely uniform and of low turbulence intensity. Additional information on this tunnel may be found in Reference 9.

This tunnel was recently extensively modified for performing aeroacoustic tests. Carmargo, Smith, Devenport and Burdisso[9] explain how the original walls of the test section were replaced with tensioned sheets of woven Kevlar, which allow sound to pass through with very little attenuation, but largely confine the air flow in the tunnel. Anechoic chambers are located behind each of the Kevlar windows to fully confine the flow and provide space for mounting acoustic measuring equipment. Carmargo *et al*[9] also describe the extensive calibration that was performed on the tunnel to confirm that the modification did not degrade the original high quality flow. Ongoing efforts continue to quiet the tunnel and thus permit more accurate measurements of the noise produced by test airfoils.

The facility is capable of acquiring aerodynamic loads on the test airfoil (through the use of airfoil surface pressure ports and a wake rake), detailed hot-wire measurements in the trailing edge boundary layer and detailed acoustic source data (via use of a 63 microphone phased array).

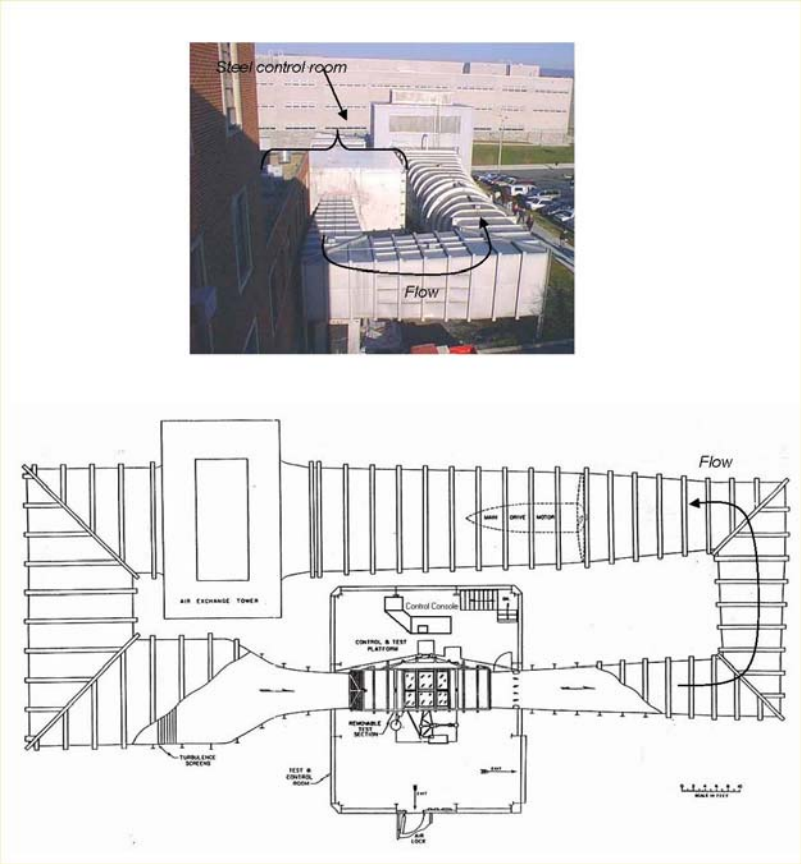

Figure 4: Virginia Tech Stability Wind Tunnel

B. Models

The airfoils tested were the DU97-W-300, developed by TU Delft for use in the root region of a wind turbine,[5,6] and a flatback version of that same airfoil; see Figure 5. The DU97-W-300 was given a nominally "sharp" trailing edge thickness of 1.7% to approximate the geometry that might result from a typical mass production manufacturing operation. The flatback version of this airfoil incorporated a 10% trailing edge thickness. Adding a simple splitter plate with a streamwise length equal to the flatback thickness and a straight trailing edge, such as that shown at the extreme left of Figure 3, to the flatback model created a third airfoil configuration.

The two airfoil models used in this test were fabricated by Novakinetics, Inc. of Flagstaff, AZ. Both were 0.91 m (36 in) in chord and 1.83 m (6 ft) in span. The nominally sharp trailing edge became 1.6 cm (0.625 in) thick, and the 10% flatback trailing edge became 9.1 cm (3.6 in) thick. The models were constructed with a 8.9 cm (3.5 in) diameter, 6.4 mm (0.25 in) wall steel tube running the entire span at ¼ chord and extending approximately 16.25 cm (6 in) beyond each end of the airfoil. This tube provides the necessary strength to withstand the aerodynamic load and serves as the wind tunnel mounting points. Internal airfoil construction details include six steel ribs welded to this tube with the spaces between the ribs filled with polyurethane foam. A fiberglass shell of approximately 2.54 mm (0.1 in) thickness forms the surface of the model. Figure 6 shows the internal construction of the flatback model.

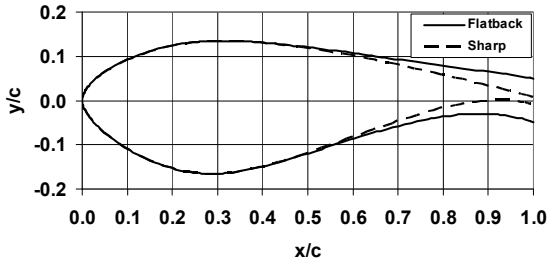

Figure 5: Airfoil profiles used for this test

The DU97-W-300 model contains 81 surface pressure taps near mid span. Of these, 40 are located on the pressure side, 39 are located on the suction side, an additional one is located on the leading edge and the final one is located on the trailing edge. The flatback model contains 82 surface pressure taps near mid span. Of these, 40 are located on the pressure side, 40 are located on the suction side, and the final two are located on the leading edge (none are located on the flat trailing edge). Each pressure tap is nominally 0.794mm (0.0313in) in diameter. Tygon tubing is attached to the taps and routed through the mounting tube to connect to the data acquisition system outside the wind tunnel. Figure 7 is a photograph of the cross section of the flatback model, while Figure 8 is a photograph of the same model with the splitter plate attached. Measurements to determine the accuracy of the model shapes will be conducted in the near future.

Figure 6: Model internal construction details.

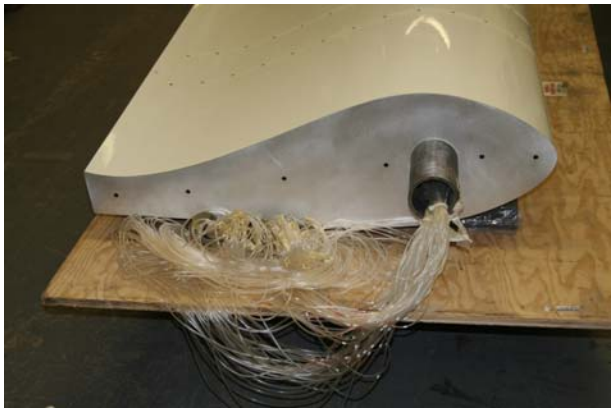

Figure 7: Flatback wind tunnel model.

Figure 8: Flatback wind tunnel model with splitter plate attached.

C. Test Methodology

The models were inserted through the floor of the test section and were mounted vertically, as illustrated in Figure 9. Model angle of attack was adjusted for tunnel blockage effects and was set manually.

All measurements were obtained with the airfoil stationary. The model angle of attack was set, the tunnel operating speed was brought up to the appropriate levels for the Reynolds numbers of interest and the required measurements were obtained at each Reynolds number. The tunnel speed was then brought down to nearly zero, the angle of attack was changed and the procedure was repeated.

Figure 9: DU97-W-300 model in wind tunnel test section. View is upstream.

Although the wind tunnel is capable of operating at Reynolds numbers (based on model chord) as high as about 5 X 10^6 for this size model, concern about the effect of extreme velocities on the Kevlar acoustic windows (especially with the vortex shedding that was expected from the flatback airfoil) limited the maximum nominal Reynolds numbers for this test to 3.2 X 10^6. Tests were also conducted a lower nominal Reynolds numbers of 1.6 X 10^6 and 2.4 X 10^6 in order to evaluate the scaling of noise generation with flow velocity.

The pressures from the model surface taps were measured with a Scanivalve system. Wake pressures were measured with a single Pitot static probe mounted on a traversing mechanism near the airfoils mid span. All pressure measurements were 1-second averages of data acquired at 1000 Hertz.

Data acquired for the aeroacoustic characterizations included microphone phased-array data, hot-wire traverses of the airfoil boundary layers, both just upstream and just downstream of the trailing edge, and a limited amount of hot-wire spectral data. The acquisition of hot wire data near the surface of the flatback airfoil proved to be especially difficult – the extremely turbulent wake generated high loads on the probe support, resulting in large-amplitude probe tip vibration. This vibration, in turn, resulted in impacts of the tip on the model and subsequent breakage of the hot wire.

The microphone phased array, shown in Figure 10, was located in the anechoic chamber on the right side of the test chamber (looking upstream), with the plane of the array vertical and parallel to the test section center line. The array consisted of 63 microphones; 9 microphones located along each of 7 arms. The custom-built microphones utilized 6.4 mm (0.25 in) diaphragm Panasonic WM-60A Electret Condenser Microphone (ECM) cartridges as the sensing elements, coupled with passive signal conditioning circuitry. All 63 microphones are sampled simultaneously at 25,600 Hz to acquire close to one million samples for each microphone for each combination of test configuration and tunnel condition.

Data were obtained for both smooth airfoil and boundary layer trip configurations, referred to subsequently as "clean" and "tripped" conditions. The boundary layer trip consisted of 5 mm wide, 0.5 mm thick zig-zag serrated tape running the entire span of the model, placed at 5% chord on the suction side of the model and at 10% chord on the pressure side of the model.

The initial test goal was to acquire both aeroacoustic and aerodynamic data for all three model configurations at the three Reynolds numbers mentioned above, at several angles of attack ranging from just below C_{dmin} to just above C_{lmax} (as predicted by a CFD code) for both clean and tripped conditions. Time constraints precluded obtaining complete data at all of these conditions. Table 1 lists the conditions at which data were obtained for the clean airfoil, flatback and flatback with splitter plate configurations.

Figure 10: Microphone phased array.

III. Aerodynamic Performance

Three typical surface pressure data distributions are presented in Figures 11-13. These distributions are only a small subset of the distributions that were obtained. These have been selected for presentation because they are high lift conditions and these results demonstrate the type of performance that can be achieved with flatback airfoils.

Figure 11 is the pressure distribution for the DU97-W-300 airfoil at 12° angle of attack at a Reynolds number of 3.2×10^6, with no boundary layer trip. Notice that there is a significant leading edge pressure peak and the airfoil has not yet reached stall conditions.

Measurements Obtained in Sandia Test

DU97-W-300 Airfoil							
Configuration			Measurements				
Effective Angle of Attack	Boundary Layer Trip	Chord Reynolds Number	Phased Array Microphones	Model Pressure Distribution	Wake Pressures	TE Hot-wire Bounday Layer Profile	TE Hot-wire Spectra
4	None	$1.6x10^6$					
4	None	$2.4x10^6$	X	X			
4	None	$3.2x10^6$	X	X	X	X	X
8	None	$1.6x10^6$	X	X	X	X	X
8	None	$2.4x10^6$	X	X			
8	None	$3.2x10^6$	X	X	X	X	X
12	None	$1.6x10^6$					
12	None	$3.2x10^6$	X	X		X	X
4	Tripped	$1.6x10^6$					
4	Tripped	$3.2x10^6$	X				
8	Tripped	$1.6x10^6$	X			X	X
8	Tripped	$2.4x10^6$	X	X			
8	Tripped	$3.2x10^6$	X	X		X	X
	Pressure side only						
	Suction side only						

DU97 Flatback							
Configuration			Measurements				
Effective Angle of Attack	Boundary Layer Trip	Chord Reynolds Number	Phased Array Microphones	Model Pressure Distribution	Wake Pressures	TE Hot-wire Bounday Layer Profile	TE Hot-wire Spectra
4	None	$1.6x10^6$	X				
4	None	$2.4x10^6$	X	X			
4	None	$3.2x10^6$	X	X	X		
10	None	$1.6x10^6$	X	X	X		
10	None	$2.4x10^6$	X	X			
10	None	$3.2x10^6$	X	X	X		
12	None	$1.6x10^6$	X				
12	None	$2.4x10^6$		X			
12	None	$3.2x10^6$	X	X	X		
4	Tripped	$1.6x10^6$		X			
4	Tripped	$2.4x10^6$		X			
4	Tripped	$3.2x10^6$		X			
10	Tripped	$1.6x10^6$	X	X			
10	Tripped	$2.4x10^6$	X	X			
10	Tripped	$3.2x10^6$	X	X	X		
12	Tripped	$2.4x10^6$		X			
12	Tripped	$3.2x10^6$		X			

DU97 Flatback--Splitter Plate							
Configuration			Measurements				
Effective Angle of Attack	Boundary Layer Trip	Chord Reynolds Number	Phased Array Microphones	Model Pressure Distribution	Wake Pressures	TE Hot-wire Bounday Layer Profile	TE Hot-wire Spectra
4	None	$1.6x10^6$	X				
4	None	$2.4x10^6$	X	X			
4	None	$3.2x10^6$	X	X	X		
10	None	$1.6x10^6$	X				
10	None	$2.4x10^6$	X	X			
10	None	$3.2x10^6$	X	X	X		
12	None	$1.6x10^6$					
12	None	$3.2x10^6$					
4	Tripped	$1.6x10^6$		X			
4	Tripped	$2.4x10^6$		X			
4	Tripped	$3.2x10^6$	X	X			
10	Tripped	$1.6x10^6$	X	X			
10	Tripped	$2.4x10^6$	X	X			
10	Tripped	$3.2x10^6$	X	X			

Table 1. Test conditions at which data were obtained.

Figure 12 presents the pressure distribution for the flatback airfoil at 10° angle of attack at a Reynolds number of 3.2 X 10^6, with boundary layer trips. The leading edge pressure peak is somewhat lower than that for the sharp airfoil, but there is no indication that this airfoil has started to stall at this condition. Note the difference between this airfoil and the sharp airfoil in the pressure distribution near the trailing edge. The pressures on the two surfaces do not blend smoothly together in this case – there is a very abrupt jump, indicative of the fact that some of the pressure recovery is occurring off the trailing edge of the airfoil, in the wake.

Figure 13 presents the pressure distribution for the flatback airfoil with splitter plate at 10° angle of attack at a Reynolds number of 3.2 X 10^6, with boundary layer trips. The pressure distribution over the entire airfoil is very similar to that for the flatback airfoil, but there are differences from mid chord aft. The pressure distribution there appears to be somewhere in between that of the flatback and that of the sharp airfoil. Again, some of the pressure recovery occurs in the wake.

IV. Aeroacoustic Results

A. Beam Forming

While it may be a simple matter to determine whether one airfoil creates more noise than another, it is much more difficult to identify the regions of an airfoil that are responsible for the creation of airfoil noise. However, without this knowledge, it is very difficult to modify the airfoil design to make it quieter.

The state of the art for noise source identification today is the microphone phased array; a large number of microphones arranged in a specific pattern. These microphones are sampled simultaneously to map a sound field and create a "sound picture". The ability of this technique to identify sound sources is directly influenced by the number of microphones used – using more microphones permits the identification of lower level sound sources. The high cost of the many good quality microphones required for this technique made it too expensive for all but large companies until recently. Now, thanks to the development of high-quality, low-cost microphone components, equipment cost have dropped dramatically. This cost reduction, coupled with improvements in analysis techniques that yield more accurate source identification with fewer microphones, has made this technique affordable for everyone. The data analysis compares the signals within a specified frequency band for all the microphones and utilizes the delay times required for sound from a potential source to reach each of the microphones to identify the actual location of each sound source. This process is typically known as "beam forming". The resolution of this technique is pretty poor below 500 Hz, so no data are acquired or reduced at frequencies below that level.

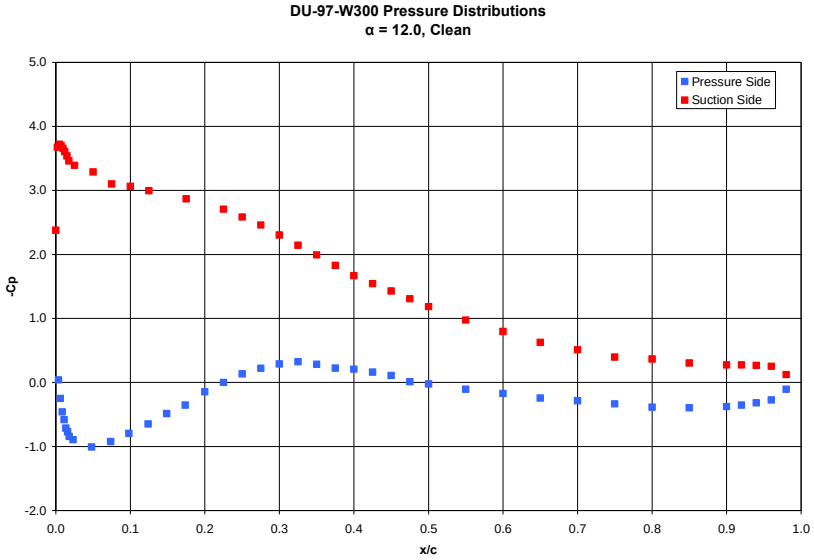

Figure 11: Surface pressure distribution for DU97-W-300 model at 12° angle of attack

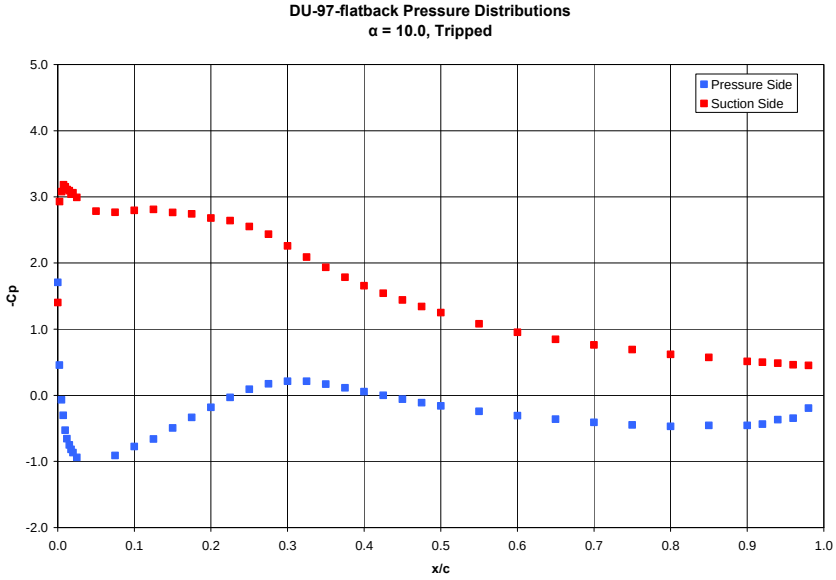

Figure 12: Surface pressure distribution for flatback model at 10° angle of attack

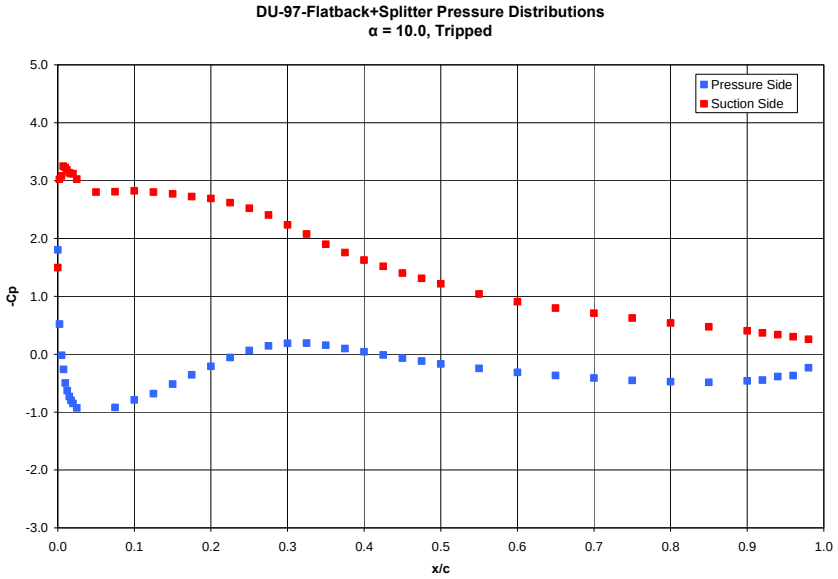

Figure 13: Surface pressure distribution for flatback model with splitter plate at 10° angle of attack

As mentioned above, at each test condition, the 63 microphones were sampled simultaneously at 25,600 Hz to acquire 8192 samples of data in each of 100 blocks for each microphone. Fast Fourier Transforms (FFTs) were performed on each block of data to determine the spectral content of that block. The spectra for all 100 blocks of data were then averaged to determine the mean spectrum for that particular microphone for that particular set of tunnel conditions and test configuration.

The data presented below are only a small subset of the data obtained. These data are all for an angle of attack of 4° at a Reynolds number of 3.2 X 10^6. The data presented are very preliminary, and future reports will present will describe more results.

Beam forming results for the DU97-W-300 are presented in Figures 14 and 15 for the clean and tripped boundary configurations, respectively. Each panel in these figures is a plot of the noise sources in the near vicinity of the airfoil at the frequency noted below the panel. 542 Hz is the lowest frequency at which data have been reduced, and the results at frequencies above 1024 Hz show very little, if any, differences. The flow is from right to left, and the leading and trailing edges of the airfoil are denoted by the vertical lines in the panels. Each panel has a sound intensity color scale just below it. Note that the color scale changes from panel to panel – the program always plots the highest sound intensity as red. While a cursory look at these figures reveals some differences between the configurations for frequencies from 683 to 767 Hz, a closer inspection of the data shows that the clean configuration sound intensity is significantly higher than that of the tripped boundary layer configuration over this frequency band. In fact, that frequency band generates a sound intensity that is several dB higher than any other frequencies included in these figures. We do not yet understand why the plots for 724 and 767 Hz show a noise source forward of the leading edge. However, the boundary layer trip evidently eliminates that noise source and the noise intensity for the tripped boundary layer configuration is very uniform over this entire frequency range.

Figure 16 presents the beam forming results for the clean flatback configuration. Those intensity levels are all much higher than the levels for the sharp trailing edge configuration. The individual plots show that the higher level noise, as expected, is generated by the trailing edge.

The impact of the addition of the splitter plate on noise generation in this frequency range may be seen in Figure 17. The sound intensity levels have returned to those found in Figures 14 and 15 for the sharp airfoil. This does not mean that this airfoil is as quiet as the sharp trailing edge airfoil; it simply means that there is comparable noise generated by this airfoil in the frequency range shown. Addition of a boundary layer trip to the splitter plate configuration results in very little change, so beam forming results for that configuration are not presented in this paper.

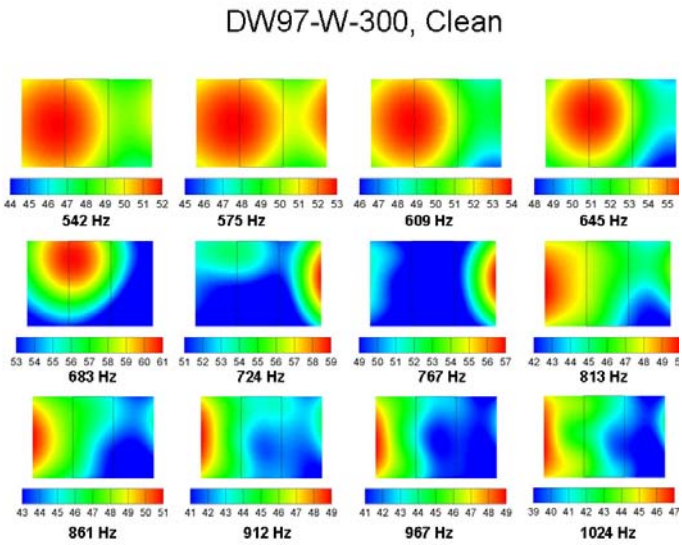

Figure 14: Beam form maps for the DU97-W-300 airfoil with no boundary layer trip. Airfoil leading and trailing edges are indicated by the vertical lines. Flow is from right to left.

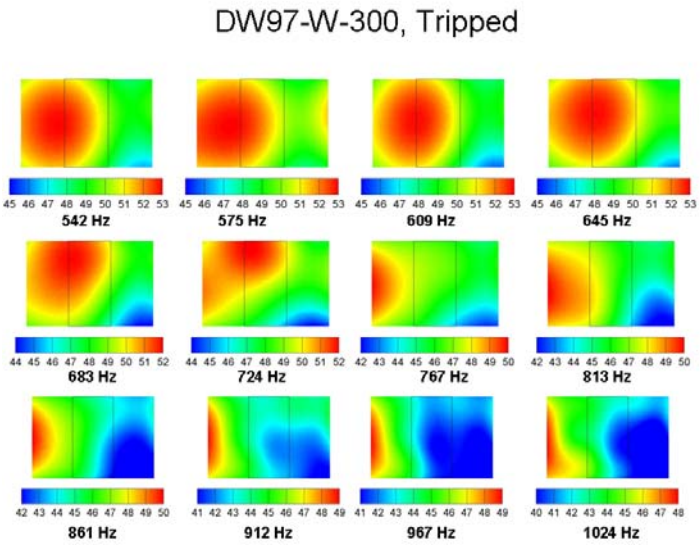

Figure 15: Beam form maps for the DU97-W-300 airfoil with boundary layer trip. Airfoil leading and trailing edges are indicated by the vertical lines. Flow is from right to left.

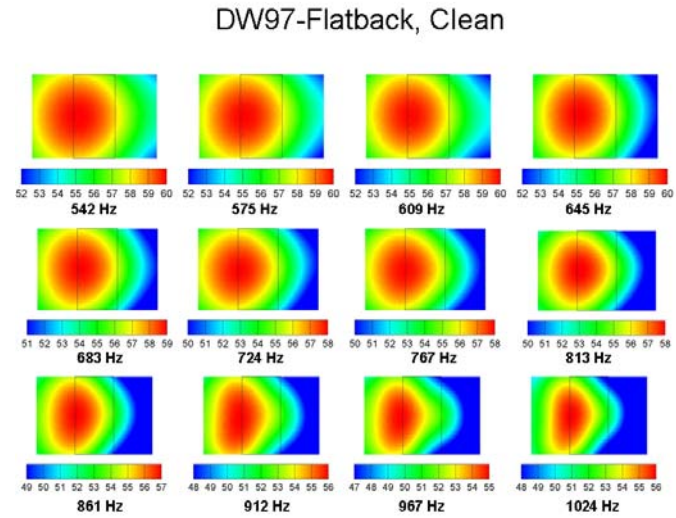

Figure 16: Beam form maps for the DU97 Flatback with no boundary layer trip. Airfoil leading and trailing edges are indicated by the vertical lines. Flow is from right to left.

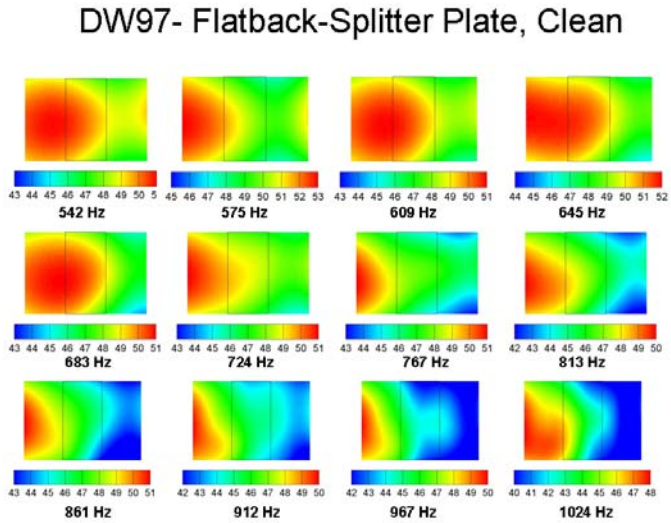

Figure 17: Beam form maps for the DU97 Flatback-Splitter Plate with no boundary layer trip. Airfoil leading and trailing edges are indicated by the vertical lines. Flow is from right to

B. Noise spectra

As mentioned above, the noise spectra that result from the FFT operations on the acoustic array data are averaged to determine a mean spectrum for each microphone in the array. These spectra yield more information on actual noise levels than do the beam forming plots presented above, as it is the integration of these spectra that yield the actual perceived noise generated by the airfoil. Noise spectra results for all three airfoil configurations with no boundary layer trip are presented in Figure 18. It is obvious from these data that the flatback configuration generates much, much more noise than the DU97-W-300 airfoil, especially in the 100-200 Hz frequency band. While the splitter plate decreases the noise level to very close to the DU97-W-300 airfoil level at most frequencies, that level is still well above the DU97-W-300 airfoil level in the 100-200 Hz band. These results certainly mirror the noise levels observed during the actual test. While the noise generated by the sharp airfoil was not discernable above the noise of the tunnel, that generated by the flatback configuration was easily heard, even outside the tunnel building. The addition of the splitter plate resulted in a significant decrease in the noise, but not down to the level of the sharp airfoil.

The impact of boundary layer trip on the noise spectra is illustrated in Figure 19. The overall character of the spectra is little changed, but the level is decreased slightly over the entire frequency range. In particular, there is a noticeable decrease in level in the vicinity of 600-800 Hz, as noted in the examination of the respective beam form plots, above.

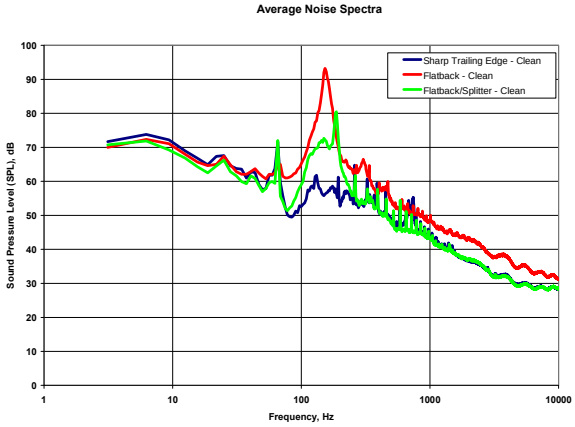

Figure 18: Integrated spectrum in for all three model configurations, no boundary layer trip.

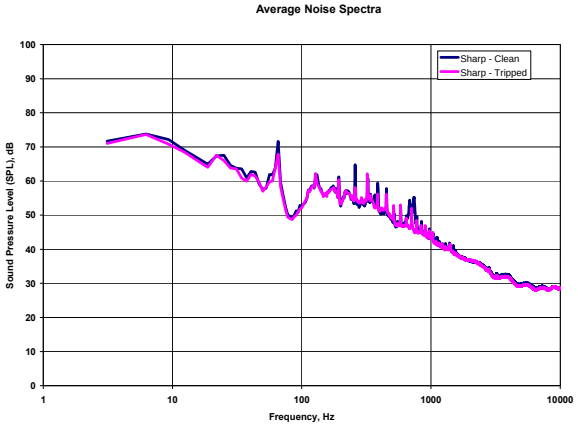

Figure 19: Integrated spectrum for DU97-W-300 airfoil.

V. Future Direction

As mentioned earlier, the data presented here is preliminary and represents a very limited portion of the data obtained in this test. Considerable effort will be devoted to reducing all of the data and ensuring that experimental bias has been eliminated to the extent possible. Once that is accomplished, additional analysis will commence and reported.

Once the experimental data have been examined to ensure that the angle of attack and pressure data are correct, predictions will be made with several CFD codes for both two-dimensional and three-dimensional geometries for both steady and unsteady conditions. Particularly emphasis will be placed on reconciling the experimental and analytical results for the most benign case of the conventional DU97-W-300 at low angles of attack with no boundary trip. If the codes can not handle that case, there is no hope that they will be able to accurately predict performance for any of the more aggressive cases.

The hot wire data from the boundary layer surveys has not been examined in this paper. The velocity and spectral data obtained from those surveys will serve to define the boundary layer conditions which provide the

driving factors for trailing edge noise generation. This information, together with the acoustics data, will be used for future validation of an aeroacoustic code now under development at Pennsylvania State University.

The acoustic data will be carefully examined and adjusted as necessary to account for background wind tunnel generated noise. Extraneous peaks in the spectral results will be identified and removed. The noise generation dependence of the three mode configurations on Reynolds number and angle of attack will be analyzed in detail. We will attempt to extend the existing empirical correlations of trailing edge (bluntness) noise proposed by Brooks, *et al*[4] to the 10% thickness ratio of this test, an order of magnitude beyond the range of data used to develop that correlation.

Finally, we will utilize the data acquired in this test to compare the noise that might be expected to be generated by a turbine blade incorporating flatback airfoils (such as the BSDS blade shown in Figure 1) with that generated by more conventional airfoils.

Now that we have the models, it would be fairly simple (all we need is funding) to run additional tests on the current configurations to full out the measurement matrix with additional data at existing angles of attack and add more angles of attack. We are also considering looking at other splitter plate configurations to see if any are more effective at reducing noise generation.

VI. Conclusions

Wind tunnel tests were conducted at nearly full-scale Reynolds number conditions to directly compare the aerodynamic and aeroacoustic performance of conventional and flatback airfoils designed for use in the root section of a wind turbine rotor. The effect on noise generation and aerodynamic performance of adding a simple trailing edge splitter plate to the flatback airfoil were also determined. Data obtained in the tests included surface and wake pressure measurements, hotwire boundary layer surveys and microphone phased array acoustic data. Data were obtained at Reynolds numbers, based on chord length, of 1.6×10^6, 2.4×10^6 and 3.2×10^6, for angles of attack from 4° to 12°, both with a clean airfoil surface and with tripped boundary layers.

Preliminary predictions from a conventional CFD code, utilizing the Spalart-Allmares turbulence model, of airfoil aerodynamic performance do not correlate well with the experimental data. Additional work is needed to resolve the reasons for the discrepancies.

The acoustics data show that, as expected, the flatback airfoil generates far more noise at these Reynolds numbers than does a conventional, sharp trailing edge airfoil. A simple, straight trailing edge splitter plate attached to the trailing edge of the flatback is very effective at reducing the noise generated by the flatback down to a level near that of the noise generated by the sharp airfoil.

Considerable additional work will be required to complete reduction of data obtained during from this test. The reduced data will be used to extend existing correlations of trailing edge noise generation, to estimate the difference in noise generation due to the use of flatbacks in a blade design, and to validate computational fluid dynamics and aeroacoustic analytical codes.

VII. References

1. Berry, Derek, 2007, "BSDS-II Final Project Report", (Currently in review), Sandia National Laboratories, Albuquerque, NM.
2. Standish, Kevin J., 2003, *Aerodynamic Analysis of Blunt Trailing Edge Airfoils & A Microtab-Based Load Control System*, M.S. Thesis, University of California, Davis, CA.
3. Ashwill, T, and Laird, D, "Concepts to Facilitate Very Large Blades, 2007, *Proceedings, ASME/AIAA Wind Energy Symposium*, Reno, NV.
4. Brooks, Thomas F.; Pope, D. Stuart; and Marcolini, Michael A., 1989." Airfoil Self-noise and Prediction", NASA RP 1218.
5. Baker, J.P., van Dam, C.P., and Gilbert, B.L., 2007, "Flatback Airfoil Wind Tunnel Experiment", (Currently in review), Sandia National Laboratories, Albuquerque, NM.
6. Paquette, J.A. and Veers, P.S, 2007, "Increased Strength in Wind Turbine Blades through Innovative Structural Design", *Proceedings, European Wind Energy Conference*, Milan, Italy.
7. Timmer, W.A., and van Rooij, R.P.J.O.M., 2003, *Summary of the Delft University Wind Turbine Dedicated Airfoils*, J. Solar Energy Engineering, Vol. 125, Nov. 2003, pp. 488-496
8. van Rooij, R.P.J.O.M., and Timmer, W. A., 2003, *Roughness Sensitivity Considerations for Thick Rotor Blade Airfoils*, J. Solar Energy Engineering, Vol. 125, Nov. 2003, pp. 497-????

9. Carmargo, H.E., Smith, B. S., Devenport, W.J., and Burdisso, R.A., 2005, “Evaluation and Calibration of a Prototype Acoustic Test Section for the Virginia Tech Stability Wind Tunnel”, Report VPI-OAE-294, Virginia Polytechnic Institute and State University.